AIAA 80-0035R

Aluminum Oxide Particle Size for Solid Rocket Motor Performance Prediction

R.W. Hermsen*
United Technologies Corporation, Sunnyvale, Calif.

A new method for predicting aluminum oxide particle size was developed for use in the Air Force Improved Solid Performance Program (SPP). Theoretical models of particle growth and breakup in rocket nozzles were compared with available particle size data. It was found that no adequate theoretical model existed to relate particle size to propellant composition and motor parameters; therefore, an empirical approach was adopted using linear and nonlinear least-squares methods. Correlations were attempted with parameters, groupings, and functional forms suggested by the theoretical models. A relatively simple model employing only three free parameters was recommended for use in SPP.

Nomenclature

a = speed of sound
C_D = drag coefficient
D_c = critical diameter for breakup
D_i = diameter of particles in *i*th class
D_0 = diameter before breakup
D_t = nozzle throat diameter
D_{43} = mass-weighted average diameter
d_p = particle diameter
I_{sp} = specific impulse
n_i = number of particles in *i*th class
n,m = generalized exponents
$\dot{m}$ = motor mass flow rate
P = pressure
Re_c = particle Reynolds number based on a_c
Re_t = Reynolds number at nozzle throat
R_c = nozzle throat radius of curvature
R_t = nozzle throat radius
S = $\rho_c D_t/\rho_p d_p$ = dimensionless scale parameter for two-phase flow
s = estimate of standard deviation
T = temperature
Δu = magnitude of particle-gas velocity difference
V_c = chamber volume
α,β = generalized coefficients
ξ = aluminum oxide concentration, g-mole/100 g
μ_g = gas viscosity
ρ_g = gas density
ρ_L = liquid density
σ = standard deviation of $\log_{10}D$; surface tension
τ = $\rho_c V_c/\dot{m}$ = chamber residence time

Subscripts

c = chamber conditions
p = particle

Superscript

$\bar{(\ )}$ = average quantity

Introduction

PARTICLE-GAS thermal and velocity lags in the nozzle represent an important source of performance loss for solid rocket motors that use aluminized propellants. Analytical methods for predicting these two-phase flow losses have been developed[1,2] and are widely used as part of an overall performance prediction methodology for motor design, propellant selection, and data interpretation.[3-5] Recent applications of performance prediction methodology are discussed in Refs. 6-8.

It is generally recognized that one of the most important variables determining two-phase flow losses is the size of the condensed aluminum oxide particles in the nozzle flow. Therefore, the accuracy of the performance prediction depends on the accuracy with which the particle size is known. In general, particle size data will not be available for any particular case of interest so that it is necessary to predict particle size based on motor and propellant variables. This paper reports the results of a study leading to a new method for predicting aluminum oxide particle size. The method was developed for use in the Improved Solid Performance Program (SPP), the Air Force standard performance prediction code for solid motors.

Particle size data, models, and correlations available up to 1975 are reviewed in Ref. 3. The problems in modeling and correlating particle size remain nearly the same at the present time. That is, there is no adequate theoretical model relating particle size to propellant and motor parameters and there are often significant differences between data reported by different investigators.

The lack of a quantitative theoretical model dictates the use of a semiempirical or wholly empirical method for correlating particle size. Two basically different approaches have been followed in the past. The first approach involves correlating experimental particle size data with motor and propellant variables, as was done in the original SPP effort.[3] This approach has the advantage of being based on independent experimental data, but data scatter may cause problems. It may also be argued that particles collected in the motor exhaust are not truly representative of those existing in the flow inside the nozzle.

The second approach involves calculating the particle size based on a critical Weber number for maximum stable drop size. Since the critical value of Weber number is not known a priori with sufficient accuracy, it is adjusted on the basis of comparisons between predicted and experimental I_{sp} values. The method has the advantage of avoiding problems associated with particle size data scatter; however, its accuracy depends on how well a single value for critical Weber number can correlate data for widely differing motors. This may not be possible, since droplet breakup is known to depend on rates of shear loading and droplet deformation as well as on Weber number.[9] A more serious disadvantage of this approach is that the sum of all errors in the other loss predictions is built into the calculated two-phase loss as a correction. Therefore, significant errors may result when

---

Presented as Paper 81-0035 at the AIAA 19th Aerospace Sciences Meeting, St. Louis, Mo., Jan. 12-15, 1981; submitted March 6, 1981, revision received July 8, 1981.

*Chief, Kinetics and Combustion, Research and Advanced Technology Department, Chemical Systems Division. Associate Fellow AIAA.

Table 1 Al_2O_3 particle size data summary

Item No.	Motor	Propellant	% Al	ξ_c	T_c, °R	$\bar{P}_c$, psia	D_t, in.	R_c/R_t	$\bar{\tau}$, msec	D_{43}, μm	σ**	Collection Method	Measurement Method	Reference
1.*	156-5	LPC-580A 87% solids PBAN	18	0.32	6260	667	60.4	0.5	113	10.9	0.22	1	OM	12,13,14
2.*	156-6	LPC-580C 87% solids PBAN	18	0.32	6260	664	34.5	0.6	110	11.1	0.22	1	OM	12,13,14
3.	156-7	TP-H8163 86% solids PBAN	16	0.26	6110	560	20.0	3.0/1.0	143	10.8	0.205	2	OM	12,13,14
4.	156-9	TP-H1115 87% solids PBAN	18	0.32	6400	560	34.5	0.9/0.8	110	12.0	0.25	2	OM	13,14
5.	TCC-120	TP-H1085 88.5% solids CTPB	20	0.34	6260	700	24.5	0.9/0.5	162	11.1	0.20	2	OM	12,13
6.*†	TCC-120	TP-H1077 86% solids PBAN	16	0.26	6110	--	21.3	--	--	8.6	--	2	OM	12
7.	UA-1205	UTP-3001 84% solids PBAN	16	0.285	5960	550	37.7	0.4	175	12.0	0.17	2,5,6	OM,SM	12,15,16
8.	260-SL2	ANB-3105 85% solids PBAN	15	0.26	5990	489	71.0	1.0	202	12.9	0.22	1	OM	12,13
9.*	260-SL3	ANB-3254 85% solids PBAN	15	0.26	5990	559	89.1	0.7	143	13.3	0.23	2	OM	13,14
10.	44SS4	ANB-3254 85% solids PBAN	15	0.26	5990	495	15.5	0.75/1.0	23	8.89	--	2	OM	13
11.*	Poseidon/FS	TP-H1114 86% solids PBAN	16	0.26	6170	870	11.6	1	116	8.75/6.2	--	2	OM	13
12.*	MM/SS-Wing II	ANP-2864 82% solids PU	17	0.293	6090	460	8.5	3	60.3	5.8	--	2	OM	13
13.	Super BATES	UTP-18,803A 90% solids HTPB	21	0.357	6670	1,000	8.0	2	74	5.23	0.35	5	SI	17
14.	MM/FS 65-in.	TP-H1011 86% solids PBAN	16	0.26	6120	650	7.5	1	91	8.98	0.35	2	OM	12
15.	45-in.	UTP-15,908 90% solids HTPB 25% HMX	18	0.305	6320	950	4.14	4	145	6.23	0.24	5	SM	22
16.	C4/TS ADP	UTP-15,908 90% solids HTPB 25% HMX	18	0.305	6320	1,000	4.04	4	90	6.17	0.21	5	SM	22
17.	MX/SS ADP	PEG/FEFO 84% solids	18	0.297	6770	1,250	6.91	2/1	157	5.77	0.21	5,8	SI	14
18.†	76-in.	ANB-3238	--	--	--	--	--	--	--	6.10	--	2	OM	13
19.†	Shuttle Staging Motor	UTP-19,048 86% solids HTPB	2	0.036	5390	1,700	3.2	1.5	6.5	1.14	0.18	5	SM	22
20.	CSD-TM-3	UTP-15,151 90% solids HTPB 25% HMX	18	0.310	6280	770	2.3	2	54	5.33	0.22	4	SM	22
21.	CSD-TM-3	UTP-15,151 90% solids HTPB 25% HMX	18	0.305	6320	1,093	2.04	2	69	4.38	0.32	5	SM	22
22.	CSD-TM-3	UTP-15,908 90% solids HTPB 25% HMX	18	0.305	6320	980	2.03	2	69	5.36	0.21	5	SM	22
23.*	70-lb BATES	RH-P-112 45% solids CMDB	20	0.271	6140	1,200	2.1	2	16	2.63	--	2	EM	13
24.†	70-lb BATES	RH-P-112 45% solids CMDB	20	0.271	5980	400	3.73	2	5.2	5.41	--	2	EM	13
25.	70-lb BATES	ANP-2969 75% solids PU	20	0.34	6440	1,000	1.48	2	35	2.32	--	2	EM	13
26.†	70-lb BATES	ANB-3066 88% solids CTPB	15	0.25	6290	1,000	1.76	2	27	1.93	--	2	EM	13
27.	70-lb BATES	TP-H-1120 86% solids PBAN	16	0.26	6125	500	3.21	2	6.9	2.72	--	2	EM	13
28.*	70-lb BATES	TP-H-8163 86% solids PBAN	16	0.26	6240	1,000	2.00	2	18	2.11	--	2	EM	13
29.	70-lb BATES	TP-H-8163 86% solids PBAN	16	0.26	6110	550	2.46	2	12	2.00	--	2	EM	13
30.*	70-lb BATES	LPC-580A 87% solids PBAN	18	0.32	6330	1,000	2.52	2	13	2.66	--	2	EM	13
31.	9C7.5-17.1	RH-P-178 56% solids CMDB	21	0.36	6670	1,000	1.70	2	17	2.60	--	2	EM	13
32.†	9C7.5-17.1	RH-SE-108 63% solids TVOPA	15	0.25	6380	1,000	1.70	2	16	1.90	--	2	EM	13

Table 1 Al_2O_3 particle size date summary (continued)

Item No.	Motor	Propellant	% Aℓ	ξ_c	T_c, °R	$\bar{P}_c$, psia	D_t, in.	R_c/R_t	$\bar{\tau}$, msec	D_{43}, μm	σ**	Collection Method	Measurement Method	Reference
33.*	10KS-2500	82% solids polyurethane	17	0.292	6010	1,000	1.9	2	32	4.59	--	7	EM	18
34.*	3KS-1000	82% solids polyurethane	17	0.292	6010	1,000	0.9	2	15	4.41	--	7	EM	18
35.*	↑	↑	17	0.31	5580	200	1.6	2	5	1.2	--	7	EM	18
36.			15	0.258	5900	1,000	0.9	2	15	4.35	—	7	EM	18
37.	↓	↓	19	0.326	6140	1,000	0.9	2	15	4.48	—	7	EM	18
38.*†	3KS-1000	82% solids polyurethane	3	0.052	5220	1,000	0.9	2	12	3.11	--	7	EM	18
39.*†	1KS-250	82% solids polyurethane	17	0.292	6010	1,000	0.3	2	6	0.75	--	7	EM	18
40.*†	1KS-250	82% solids polyurethane	3	0.052	5220	1,000	0.3	2	5	0.25	—	7	EM	18
41.	HI-5PC	DDP-08 41% solids CMDB	20.9	0.368	7020	1,000	0.8	2	6.5	3.12	0.390	3	OM	21
42.	↕	↕	↕	↕	6980	800	0.95	2	4.6	3.23	0.372	3	OM	21
43.	HI-5PC	DDP-08 41% solids CMDB	20.9	0.368	6920	600	1.1	2	3.4	3.21	0.402	3	OM	21
44.*	3KS-500	ANB-3254 85% solids PBAN	15	0.26	6060	1,000	1.0	0.5	3.9	2.15	—	2	EM	13
45.*	15-1b BATES	RH-P-112 45% solids CMDB	20	0.271	6100	1,000	1.28	2	8.3	2.19	--	2	EM	13
46.	CSD-TM-1	UTP-15,908 90% solids HTPB 25% HMX	18	0.305	6340	1,116	0.70	2	25	4.99	0.20	5	SM	22
47.	CSD-TM-1	UTP-15,908 90% solids HTPB 25% HMX	18	0.305	6350	1,368	0.65	2	29	4.76	0.21	5	SM	22
48.	CSD-TM-1	UTP-13,945 88% solids HPTB	18	0.315	6320	885	1.31	2	7.1	2.61	0.27	4	SM	22
49.	CSD-4 1b	UTP-11,475 88% solids CTPB	18	0.299	6470	1,000	0.625	2	11.7	3.00	0.26	4	SM	22
50.	CSD-4 1b	UTP-13,945 88% solids HTPB	18	0.315	6340	997	0.835	2	6.8	3.56	0.18	4	SM	22
51.	CSD-4 1b	UTP-15,158 90% solids HTPB 34% HMX	16.5	0.28	6130	1,000	0.578	2	13.7	2.46	0.21	4	SM	22
52.	CSD-4 1b	UTP-15,908 90% solids HTPB 25% HMX	18	0.305	6320	1,030	0.544	2	15.8	3.06	0.20	5	SM	22
53.†	CSD-3C2-X	UTP-3096 84% solids PBAN	16	0.277	6030	1,100	0.25	2	67	4.09	0.35	3	EM	19
54.	↑	↑	16	0.277	6060	1,000	0.50	2	67	4.08	0.32	3	EM	19
55.			16	0.277	5960	630	0.50	2	68	3.64	0.29	3	EM	19
56.†			16	0.270	5640	115	0.50	2	71	0.52	0.22	3	EM	19
57.			16	0.277	6030	970	0.50	2	32	3.23	0.33	3	EM	19
58.			16	0.277	5980	730	0.50	2	33	2.54	0.29	3	EM	19
59.			16	0.273	5680	140	0.50	2	35	1.04	0.24	3	EM	19
60.			16	0.277	6030	980	0.50	2	14	2.99	0.33	3	EM	19
61.			16	0.277	5970	650	0.50	2	15	2.69	0.38	3	EM	19
62.			16	0.276	5930	470	0.50	2	15	2.20	0.29	3	EM	19
63.	↓	↓	16	0.27	5640	110	0.50	2	17	0.93	0.26	3	EM	19
64.	CSD-3C2-X	UTP-3096 84% solids PBAN	16	0.274	5760	190	1.00	2	8	1.05	0.27	3	EM	19
65.	CSD-3C2-X	UTX-4574 82% solids PBAN	5	0.091	5260	600	0.50	2	15	1.05	0.31	3	EM	20
66.	2C1.5-4	UTP-13,945 88% solids HTPB	18	0.315	6340	997	0.335	2	4.1	2.46	0.25	4	SM	22

*Indicates data was included in original SPP correlation, Reference 30.

**Standard deviation of $\log_{10} D$ in log-normal distribution. Calculated from original particle counts.

† Data not used in final correlation.

Collection Method

1 RB-57 bomber with LASL sampler
2 Petri dishes
3 Closed tank
4 Brass post collector
5 CSD probe
6 U-2 with NASA sampler
7 Wetted plate collector
8 RPL box collector

Measurement Method

O optical microscope
E transmission electron microscope
S scanning electron microscope
M measured and counted manually
I image analyzer

predictions are made for motors or operating conditions different from those considered in the original correlation. Furthermore, application of the method is an iterative procedure in which lags and other conditions at the nozzle throat are calculated using an assumed particle size, the result serves as the basis for predicting a new particle size and the process is repeated until it converges.

Weighing the arguments discussed above, a method based on correlating experimental particle size data was chosen for the Improved SPP. The correlation was basically empirical; however, various theoretical models were used to provide guidance in selecting the form of the correlation.

The particular average diameter correlated was D_{43}, the mass-weighted average diameter.

$$D_{43} = \frac{\Sigma n_i D_i^4}{\Sigma n_i D_i^3} \tag{1}$$

This selection was based on the work of Smith[10] who demonstrated by means of comparative calculations that D_{43} was the most appropriate average diameter for use in predicting two-phase flow losses. Data collection and screening, a brief review of theoretical models, and the correlation task are discussed in the following sections.

Data Collection

Measurements of Al_2O_3 particle size in solid rocket motor exhausts made during the period 1962-1978 were reviewed in detail. In many cases the original raw data on particle counts and measured sizes were located and values of D_{43} and σ (standard deviation of $\log_{10}D$) were recalculated, if necessary. A first screening was conducted to exclude data of known or suspected bias, based on an evaluation of the sampling and measurement techniques and the number of particles measured. The resulting data set, shown in Table 1, included more than 60 different combinations of motor, propellant, and chamber pressure. Many of these represented several samples taken from more than one motor test and duplicate analyses of samples. This significantly expanded the data base used in the original SPP correlation,[3] which included only 16 different sets of data.

Data that were reviewed but not considered in the correlation included the early semiquantitative measurements of Brown and McArty[11] and the data contained in Refs. 23-26. The data of Sehgal[23] did not agree with later measurements made using the same closed-tank apparatus.[25] However, the later data could not be used in the present study since neither D_{43} nor the particle count data were reported. Measurements using a light-scattering technique[24,25] were apparently biased toward small particles.

Recent measurements by Strand et al. of particles in the Titan IIIC booster exhaust used a particle mobility analyzer and particle impactors with automated sizing techniques.[26,27] The mobility analyzer is inherently limited to particles less than about 1 μm in diameter; although not correspondingly limited, the reported impactor distributions also terminate at about 1 μm even though particles in the 10-μm range were observed.[27] This implies that the sizing technique may have been saturated with the submicron particles, which are present in overwhelming numbers even when insignificant on a mass basis. On the other hand, Dawbarn[28] has correctly pointed out that the earlier data[12,15,16] appear to be biased against the submicron particles in the distribution. This bias is significant with respect to important atmospheric and environmental questions but probably has little impact on the higher moments of the distribution (D_{43}) that are dominated by the larger particles.

Several references were found which reported no new data but attempted to analyze some part of the data reported in Refs. 12-25. Worster[29] analyzed the data reported by Radke[12] and proposed a particle size distribution function and a curve relating the average particle size to nozzle throat diameter. This curve is similar to the relationship proposed by Beckman[13] and is in direct conflict with the type of correlation proposed by Cheung[18] and used in the original SPP correlation,[30] which emphasizes the importance of chamber residence time. In reviewing the data available up to 1967, Brown[31] concluded that residence time might be an important factor for small motors, but nozzle throat diameter was the dominant factor for larger motors. The relative importance of residence time vs nozzle size is discussed further in the section on data correlation.

Review of Al_2O_3 Particle Size Models

Various theoretical models that have been proposed to explain Al_2O_3 particle size were reviewed in order to provide guidance in correlating the particle size data. Results of the review are summarized in Table 2.

Models of particle growth in the combustion chamber account for condensation and coagulation mechanisms. The model proposed by Fein[32] is of little use since it does not predict a mean size and only provides a size distribution once a mean size is known. The models of Cheung[18] and Jenkins[33] are more useful and suggest that the effects of pressure and aluminum concentration might be accounted for by a correlation of the form $\bar{d}_p \propto P^n \xi^m$, where values of the exponents n and m depend on the controlling mechanism. For example, Cheung's reaction-limited mechanism implies $n = m = 1/3$, whereas Jenkins' diffusion-limited mechanism implies $n = 0$, $m = 1/2$. The functional dependencies implied by Jenkins' model were basically unchanged when a simplified treatment of particle coagulation[34] was included.

The collision-coalescence models for particle growth in the nozzle imply a complex dependence of average particle size on the product $P\xi$. The models of Marble[35] and Nack[36] assume constant gas-particle velocity lag which leads to the result that particle growth is independent of nozzle throat diameter and throat radius of curvature. Later work by Crowe[37] and Jenkins[33] showed that relaxing the constant lag assumption leads to a dependency on the usual two-phase flow scaling parameters, including throat diameter and throat radius of curvature.

A model for particle breakup in the nozzle was first proposed by Bartlett and Delaney[38] based on the critical Weber number concept. In addition to Weber number, it is known that the characteristic time for breakup is important in determining whether breakup can actually occur in a given flow situation.[39] The breakup models imply a dependence on pressure, throat diameter, and radius of curvature but are independent of aluminum concentration.

Correlation of Particle Size Data

As a first step in correlating the particle size data, linear regression analyses were carried out to investigate the degree of dependence on the variables D_t, P_c, τ, R_c/R_t, T_c, and ξ_c. Correlations between the independent variables were also examined. The value of chamber residence time, τ, was based on time averages of the chamber density and mass flow rate and the empty chamber volume when half the propellant was expended. As expected, the variables D_t, ξ_c, and P_c all appeared to be significant. The correlation with D_t was stronger than with τ, contrary to the premise underlying the original SPP correlations; however, τ was a significant variable at low values of τ. The effects of τ and D_t were somewhat confounded since there was a strong correlation between these two variables. A surprising result was that throat radius of curvature, R_c, appeared to have little influence. This result must be treated with caution owing to a rather strong negative correlation between R_c/R_t and D_t in the data collection (i.e., the large nozzles had sharp throats). Chamber temperature appeared to have an influence, higher temperatures leading to smaller particles; however, the statistical significance of this dependency was questionable. In addition, there was a strong

Table 2 Proposed models for aluminum oxide particle size in rocket chamber/nozzle

Type of model	Source	Significant parameters	Critical assumptions	Significance/limitations
1) Particle growth in chamber				
a) Condensation	Fein[32]	Residence time Particle growth rate	Heterogeneous nucleation with arbitrary nucleus concentration Constant linear growth rate of a particle 1-D residence time distribution	Model only provides distribution once mean size is known
	Cheung[18]	Residence time Pressure Aluminum concentration (ξ)	Second-order kinetics with excess oxidizer Nucleation ignored Mass rate of condensation independent of diameter	Suggests mean diameter proportional to $P^{1/3}\ \xi^{1/3}$ Average $d_p^3 \propto 1-\exp(-\alpha Pt)$ where α depends on propellant
b) Condensation plus coagulation	Jenkins[33]	Residence time Pressure Aluminum concentration (ξ)	Small particle collision rates Simplified coalescence function—Golovin[34] Single nucleus size	Suggests mean diameter proportional to $P^n \xi^m$ Average $d_p^3 \propto -\exp(-f(t))$
2) Particle growth in nozzle	Marble[35]	Pressure Aluminum concentration (ξ)	Constant lag Similarity transform	Suggests that growth depends on $\rho_c a_c \bar{d}_{pc} \xi_c / \mu_g$ Independent of R_t, R_c/R_t
	Nack[36]	Same as above	Same as above	Same as above
	Crowe[37]	Pressure Throat diameter R_c/R_t	Mass of smaller particles distributed over larger classes following a collision	Rate of growth depends on $P\xi$ and two-phase flow scaling parameters: S, Re_c, R_c/R_t
	Jenkins[33]	Same as above	Maximum particle size in distribution 13 μ	Same as above
3) Particle breakup in nozzle	Bartlett[38]	Pressure Throat diameter R_c/R_t	Critical Weber number	Limiting particle size depends on $\sigma/(C_D \rho \Delta u^2)_{\max}$
	Kurzius[39]	Same as above	Critical Weber number Characteristic time for breakup	Breakup time depends on D_c/D_0, ρ_L, Δu

Table 3 Evaluation of original SPP particle size model

	Model	s	χ^2	Remarks
L7	$D_{43}=0.135 D_t^{0.291}\xi_c^{0.600}P_c^{0.484}\tau^{0.203}$	0.3851	8.75	Best linear model
N0	$D_{43}=0.454 P_c^{1/3}\xi_c^{1/3}(1-\exp(-0.1023\tau))(1+0.045D_t)$	0.6418	24.30	Original SPP model and coefficients[a]
N1	$D_{43}=1.8604 P_c^{0.2103}\xi_c^{0.3375}(1-\exp(-0.07033\tau))(1+0.02917D_t)$	0.5711	19.24	Original SPP model with new coefficients

[a] Coefficient of τ obtained from relationship $\tau/L^* = 0.0391$ ms/in.

NOTE: All coefficients are for units as follows: D_{43}, μm; D_t, in.; P_c, psia; ξ_c, mole/100 g; τ, ms; $\chi^2=\Sigma(\ln(D_{43}/D_{43\text{model}}))^2$; $s=\sqrt{\chi^2/\nu}$.

correlation of chamber temperature with aluminum level and Al_2O_3 concentration among the data.

The data were compared with the original SPP correlation using both the original set of empirical coefficients and a new set of coefficients generated from the data using a nonlinear least-squares code. These results are summarized in Table 3, together with results from the best linear model. The comparison showed that the original SPP model was inadequate, not only with respect to the value of the coefficients, but also with respect to functional form. That is, even with reoptimized coefficients it gave a significantly worse fit than a simple power-law model including the same variables.

A number of alternative models were investigated using nonlinear least-squares analyses. The theoretical models reviewed in the previous section provided guidance in selecting the functional relationships and combinations of variables to be investigated. Reynolds number was an important variable in several of the theoretical models, suggesting that Reynolds number at the nozzle throat, Re_t, might be a better correlating variable than D_t alone. The models for growth by condensation and coagulation indicated a strong interaction between the variables τ, P_c, and ξ_c, so that the particle size for large motors would be less dependent on P_c and ξ_c than for small motors. In particular, these models suggested functional dependencies of the form $P_c\xi_c(1-\exp(-\beta P_c \xi_c \tau))$ or $1-\exp(-\beta P_c D_t \tau)$. The models for growth by collision and coalescence suggested including a factor of the form $(1+\beta Re_t \xi_c)^{-1}$, and some of the data for small motors seemed to correlate with a factor $(1+\beta/P_c)^{-1}$.

Attempts to correlate the data using the ideas given above led to the conclusion that there were significant variations in D_{43} that were apparently unrelated to any of the motor and propellant variables. The data obtained by any given technique generally agreed to within ±35% about an average value. In particular, data based on samples collected using open Petri dishes appeared to be significantly lower than the data from other sampling techniques. A review of the sampling methods indicated a distinct possibility that the Petri-

Table 4 Correlation of Al_2O_3 particle size data

	Model	s
L7	$D_{43}=5.1769\ D_t^{0.2624}\xi_c^{0.5038}P_c^{0.4223}\tau^{0.1898}$	0.288
L11	$D_{43}=0.03044\ Re_t^{0.2655}\xi_c^{0.5957}P_c^{0.1719}\tau^{0.1860}$	0.287
N3	$D_{43}=0.1442\ Re_t^{0.2463}\xi_c^{0.6181}(1+108.0/P_c)^{-1}\tau^{0.1982}$	0.278
N3A	$D_{43}=4.8287\ D_t^{0.2418}\xi_c^{0.5580}(1+314.2/P_c)^{-1}\tau^{0.2008}$	0.275
N4	$D_{43}=3.8709\ D_t^{0.2292}\xi_c^{0.5981}(1-\exp(-0.003509P_c))\tau^{0.2076}$	0.269
N5	$D_{43}=10.371\ D_t^{0.3224}\xi_c^{0.6156}(1+332.6/P_c)^{-1}(1-\exp(-0.2389\tau))$	0.311
N8	$D_{43}=0.2835\ Re_t^{0.3132}\xi_c^{0.4530}P_c^{-0.1858}(1-\exp(-0.001091\xi_cP_c\tau))$	0.294
N9	$D_{43}=0.03812\ Re_t^{0.3256}(1-\exp(-0.001451\xi_cP_c\tau))$	0.308
N9A	$D_{43}=3.6304\ D_t^{0.2932}(1-\exp(-0.0008163\xi_cP_c\tau))$	0.298
N10	$D_{43}=0.03885\ Re_t^{0.3252}(1-\exp(-0.01758\xi_c^{1.819}P_c^{0.7524}\tau))$	0.294
N11	$D_{43}=0.1776\ Re_t^{0.3079}P_c^{-0.1861}(1-\exp(-0.0009740\xi_cP_c\tau))$	0.303
N11A	$D_{43}=1.8323\ D_t^{0.3076}P_c^{0.09722}(1-\exp(-0.0009695\xi_cP_c\tau))$	0.299
N12	$D_{43}=0.06232\ Re_t^{0.3303}\xi_c^{0.4606}(1-\exp(-0.001675\xi_cP_c\tau))$	0.299
N12A	$D_{43}=5.4633\ D_t^{0.2948}\xi_c^{0.3392}(1-\exp(-0.008710\xi_cP_c\tau))$	0.294
N15	$D_{43}=9.3879\ D_t^{0.2832}\xi_c^{0.6364}(1-\exp(-0.003443P_c))(1+3.480/\tau)^{-1}$	0.287
N16	$D_{43}=3.7350\ D_t^{0.2301}(1+0.2875/\xi_c)^{-1}(1-\exp(-0.003462P_c))\tau^{0.2046}$	0.267
N17	$D_{43}=18.345\ D_t^{0.2198}(1-\exp(-0.3546\xi_c))(1-\exp(-0.003748P_c))\tau^{0.2172}$	0.277

Notes: $s=\sqrt{\chi^2/\nu}$ where $\chi^2=\Sigma[\ln(D_{43}/D_{43\,\mathrm{model}})]^2$ and ν = degrees of freedom. All results with modified data set (8/78).

dish data might be biased toward smaller particles; however, there was also possible bias toward larger particles in the other data. Therefore, it was decided to assign each point equal weight in obtaining the final correlation irrespective of sampling technique. Eleven data points contained in the original set were not included in those used for the final correlation, as indicated in Table 1. Two points were deleted owing to insufficient data on motor and propellant variables. The other deleted points were believed to be in gross error since they were inconsistent with the bulk of the other data and with similar data from the same source. Sufficient documentation was available to identify specific problems that occurred in sampling and measurement for three of the deleted points. No explanation could be found for the discrepancy in the other six points.

A number of alternative models that were investigated are shown in Table 4. Models L7 and L11 are the best power-law models and Models N3-N17 involve different forms for the dependency on ξ_c, P_c, and τ. Five types of models were fit using both throat diameter, D_t, and Reynolds number at the throat, Re_t, as the correlating parameter to account for nozzle scale. A pair-by-pair comparison of these models (L7 vs L11, N3 vs N3A, N9 vs N9A, N11 vs N11A, and N12 vs N12A) indicated no significant difference in the fit.

Not shown in Table 4 are three models which include a factor of the form $(1+\beta Re_t\xi_c)^{-1}$ that were investigated. The form of this factor was suggested by the analytical studies of particle growth by collision and coalescence. In each case the nonlinear least-squares fit attempted to converge to a large negative value of β, thereby yielding negative values of D_{43} for some cases. Arbitrarily restricting β to avoid negative values of D_{43} led to poorer fits than obtained with the other models. This difficulty has been encountered previously with the simplified collision and coalescence models of Marble and Nack.

The correlation results indicated that scatter in the data would not permit obtaining a correlation with standard deviation significantly less than 0.3. At this level the goodness of fit was dominated by data scatter rather than by differences in the models; therefore, further efforts to improve the correlation would be useless. With this in mind, Model N9A was selected for use in the Improved SPP on an interim basis:

$$D_{43}=3.6304\ D_t^{0.2932}(1-\exp(-0.0008163\xi_cP_c\tau)) \qquad (2)$$

where D_{43} is the mass-weighted average diameter (μm), D_t is the nozzle throat diameter (in.), ξ_c is the Al_2O_3 concentration in the chamber (g-mole/100 g), P_c is the chamber pressure (psia), and τ is the average chamber residence time (ms).

Discussion

Equation (2) is the simplest model providing an acceptable fit of the data ($s<0.3$) and employs only three free coefficients. The standard deviation of this model, $s=0.298$, corresponding to a deviation in D_{43} of about $\pm 35\%$, is higher than desired but is commensurate with the data scatter. A number of the models using four or five coefficients gave lower standard deviations than Eq. (2); however, the improvement in fit was not statistically significant.

The form of Eq. (2) suggests the following physical interpretation. The factor involving D_t expresses the effect of nozzle scale on velocity gradients in the nozzle entrance and throat and on the corresponding shear forces leading to particle breakup.[38] According to Eq. (2) this is the mechanism controlling particle size for most full-scale motors. Throat radius of curvature also has a strong influence on velocity gradients in the nozzle throat region. The apparent insensitivity of D_{43} to R_c is believed to be a misleading result caused by the negative correlation between R_c/R_t and D_t in the data. It is likely that the effects of other variables which should have a weaker influence on particle breakup (P_c, T_c) were obscured by the data scatter. The exponential factor including the product $\xi_cP_c\tau$ in Eq. (2) expresses a limitation to particle size imposed by growth mechanisms in the combustion chamber. The form of this factor is generally consistent with models for particle growth[18,33] and the product $\xi_cP_c\tau$ may be interpreted as the ratio of residence time to the time for the particles to grow to a size where breakup in the nozzle will occur. The limitation imposed by particle growth in the chamber is only important at low values of $\xi_cP_c\tau$, corresponding to subscale motors at low pressure or having low aluminum levels.

The Improved SPP model, Eq. (2), is plotted vs D_t in Fig. 1, together with data from Table 1, the original SPP model, and two other published particle size correlations.[6,40] Only data used for the final correlation are shown, and several points with low $\xi_cP_c\tau$ values were adjusted to the stated reference conditions ($\xi_c=0.315$, $P_c=700$ psia, $\tau\geq 70$ ms) on the basis of the exponential factor in Eq. (2). Equation (2)

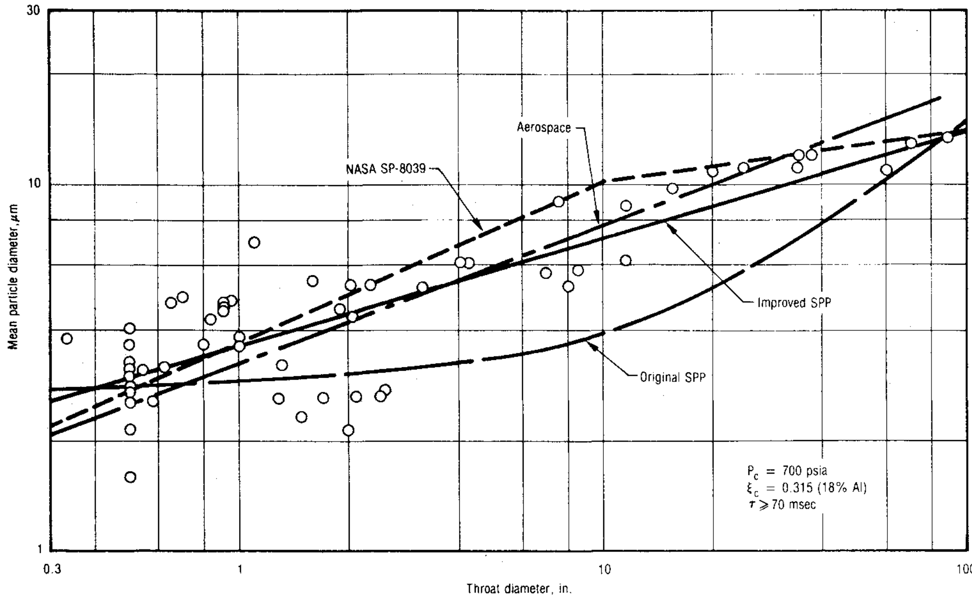

Fig. 1 Comparison of particle size correlations.

predicts significantly larger particle sizes than the original SPP model, but lies reasonably close to the correlations recommended in NASA SP-8039[40] and Ref. 6. Although in good agreement with the major trends of the data, the accuracy of Eq. (2) is open to some question owing to the data scatter. Verification of the model will, of course, ultimately depend on comparisons of predicted and measured specific impulse efficiencies.

Conclusions

1) Throat diameter, chamber pressure, and aluminum oxide concentration were the most important variables influencing particle size. There was a lesser, but still significant effect of chamber residence time at short residence times. Throat radius of curvature appeared to have no effect.

2) The original SPP particle size model was unsatisfactory, even when the coefficients were reoptimized with respect to the new data set.

3) There was significant scatter in the data owing to differences between different laboratories and techniques. This scatter did not permit obtaining a correlation with a standard deviation in mass weighted average diameter less than about 35%. At this level the goodness of fit was dominated by data scatter rather than by differences in the models.

4) A relatively simple model that employs only three free parameters and provides an acceptable fit of the data was recommended for use in SPP.

Acknowledgments

This work was sponsored by Software and Engineering Associates, Inc., under Air Force Rocket Propulsion Laboratory prime Contract F04611-77-C-0046.

References

[1]Kliegal, J.R. and Nickerson, G.R., "Flow of Gas-Particle Mixtures in Axially Symmetric Nozzles," *Detonation and Two-Phase Flow,* Academic Press, New York, 1962, pp. 173-194.

[2]Hoffman, J.D. and Lorenc, S.A., "A Parametric Study of Gas-Particle Flows in Conical Nozzles," *AIAA Journal,* Vol. 3, Jan. 1965, pp. 103-106.

[3]Coats, D.E. et al., "A Computer Program for the Prediction of Solid Propellant Rocket Motor Performance," Vol. I, Ultra-Systems, Inc., AFRPL-TR-75-36, July 1975.

[4]Daines, W.L., Mayberry, J.L., Lund, R.K., and Abel, R., "Prediction of Thrust Losses Occurring in Solid-Propellant Rocket Motors," AIAA Paper 74-1201, Oct. 1974.

[5]JANNAF Performance Standardization Working Group, Solid Performance Subcommittee, 8th Meeting Minutes, Chemical Propulsion Information Agency, July 1974, pp. 3-23.

[6]Landsbaum, E.M. and Salinas, M.P., "Solid Propellant Specific Impulse Prediction," presented at AGARD, Propulsion and Energetics Panel, 53rd Meeting, Symposium on Solid Rocket Motor Technology, Oslo, Norway, April 1979.

[7]Jacques, L., "Performance Prediction of Solid-Propellant Rocket Motors and Application to High Expansion-Ratio Nozzles," Paper 79-1295, June 1979.

[8]DeAimicis, R., Fabrizi, A., and Ricciardi, A., "Performance Prediction of Apogee Boost Motors and Correlation with Vacuum Firing Tests and Flight Results," Paper 79-1296, June 1979.

[9]Morrell, G., "Critical Conditions for Drop and Jet Shattering," NASA TN D-644, Feb. 1961.

[10]Smith, P.W., work presented at AFRPL Two-Phase Flow Conference, San Bernardino, Calif., March 1967.

[11]Brown, B. and McArty, K.P., "Particle Size of Condensed Oxides from Combustion of Metallized Solid Propellants," *Eighth Symposium (International) on Combustion,* Williams and Wilkins, Philadelphia, 1962, pp. 814-823.

[12]Radke, H.H., Delaney, L.J., and Smith, P., "Exhaust Particle Size Data from Small and Large Solid Rocket Motors," Aerospace Corporation, Contract AF04(695)-1001, Report No. TOR-1011 (S2951-18)-3, July 1967.

[13]Beckman, C.W., "Solid Propellant Impulse Scaling Prediction Techniques," AFRPL-TR-71-7, Feb. 1971.

[14]Beckman, C.W. and Geisler, R.L., Air Force Rocket Propulsion Laboratory, unpublished particle size/count data.

[15]Willoughby, P.G. and Carlson, R.L., "Sampling and Size Determination of Particles from the Titan III-C Exhaust Plume," United Technology Center, TR-33-74-U1, Feb. 1974.

[16]Ferry, G.F. and Lem, H.Y., "Aerosols at 20 Kilometers Altitude," *Second International Conference on Environmental Impact of Aerospace Operations in the High Atmosphere,* edited by A.J. Broderick, American Meteorological Society, Boston, 1974, pp. 27-33.

[17]Stephen, W.A., Warren, T.C., and Scannell, P.R., "Ballistic Missile Propellant Evaluation Test Motor System – Super BATES," CSD 2537-FR, Final Report, Contract F04611-75-C-0017, AFRPL-TR-77-5, Feb. 1977.

[18]Cheung, H. and Cohen, N.S., "Performance of Solid Propellants Containing Metal Additives," *AIAA Journal,* Vol. 3, Feb. 1965, pp. 250-257.

[19]Crow, C.T. et al., "Dynamics of Two-Phase Flow in Rocket Nozzles," United Technology Center, UTC 2102-FR, Final Report, Contract N0w264-0506-C, Sept. 1963.

[20]Crowe, C.T. et al., "Investigation of Particle Growth and Ballistic Effects on Solid Propellant Rockets," United Technology Center, UTC 2128-FR, Final Report, Contract N0w65-0222-f, June 1966.

[21]"High Energy Solid Propellant Combustion Efficiency Investigation," Hercules, Inc., Final Report AF04(611)-010814, AFRPL-TR-67-23, Feb. 1967.

[22]Willoughby, P.G. and Hermsen, R.W., Chemical Systems Division, unpublished particle size/count data.

[23]Sehgal, R., "An Experimental Investigation of a Gas-Particle System," Jet Propulsion Laboratory, Technical Report No. 32-238, March 1962.

[24]Dobbins, R.A., "Remote Size Measurements of Particulate Products of Heterogeneous Combustion," *Eleventh Symposium (International) on Combustion*, The Combustion Institute, 1967, p. 921.

[25]Dobbins, R.A., and Strand, L.D., "A Comparison of Two Methods of Measuring Particle Size of Al_2O, Produced by a Small Rocket Motor," *AIAA Journal*, Vol. 8, Sept. 1970, pp. 1544-1550.

[26]Strand, L.D. and Varsi, G., "Airborne Measurements of Particulates from Solid Rocket Boosters," JANNAF 8th Plume Technology Meeting, CPIA Publication No. 257, Sept. 1974, pp. 141-163.

[27]Strand, L.D., Bowyer, J.M., Varsi, G., Lane, E.G., and Gauldin, R., "Characterization of the Exhaust Particulates in the Ground Cloud and High Altitude Plume of Large Solid Propellant Booster Rockets," AIAA Paper 80-0354, Jan. 1980.

[28]Dawbarn, R., "Species in Solid Rocket Exhaust," ARO, Inc., Triannual Progress Report, V34P-AIA, Jan. 1977.

[29]Worster, B. and Kadomiya, R.H., "Rocket Exhaust Aluminum Oxide Particles," AIR RR-30, Special Technical Report, Contract DAAH01-71-C-1291, Aug. 1973.

[30]Coats, D.E. et al., "A Computer Program for the Prediction of Solid Propellant Rocket Motor Performance," Vol. I, AFRPL-TR-75-36, July 1975, pp. 5-9—5-14.

[31]Brown, B., "Oxide Particles in Solid Rocket Exhausts—Their Formation and Growth," Institute for Defense Analysis, Report No. IDA-HQ67-5777-3, Contract DAHC15-67-C-0011, Nov. 1967.

[32]Fein, H.L., "A Theoretical Model for Predicting Aluminum Oxide Particle Size Distributions in Rocket Exhausts," AIAA Journal, Vol. 4, Jan. 1966, p. 92.

[33]Jenkins, R.M. and Hoglund, R.F., "A Unified Theory of Particle Growth in Rocket Chambers and Nozzles," AIAA Paper 69-541, June 1969.

[34]Golovin, A.M., "On the Kinetic Equation for Coagulating Cloud Droplets with Allowance for Condensation," *Academy of Sciences USSR, Bulletin, Geophysics Series,* Oct. 1963, pp. 949-953.

[35]Marble, F.E., "Droplet Agglomeration in Rocket Nozzles Caused by Particle Slip and Collision," *Astronautica Acta,* Vol. 13, No. 2, 1967, pp. 159-166.

[36]Nack, T.H., "Theory of Particle Agglomeration, Mean Size Determination and Chamber Coagulation in Rocket Motors," *Proceedings of the AFRPL Two-Phase Flow Conference,* AFRPL-TR-67-223, Vol. I, Aug. 1967, p. 103.

[37]Crowe, C.T. and Willoughby, P.G., "A Study of Particle Growth in a Rocket Nozzle," *AIAA Journal,* Vol. 5, July 1967, pp. 1300-1304.

[38]Bartlett, R.W. and Delaney, L.J., "Effect of Liquid Surface Tension on Maximum Particle Size in Two-Phase Nozzle Flow," *Pyrodynamics,* Vol. 4, 1966, pp. 337-341.

[39]Kurzius, S.C. and Raab, F.H., "Measurement of Droplet Sizes in Liquid Jets Atomized in Low Density Supersonic Streams," NASA CR-1242, Dec. 1968.

[40]Miller, W.H., "Solid Rocket Motor Performance Analysis and Prediction," NASA SP-8039, May 1971, p. 24.